Dental Materials Journal 2023; 42(3): 351–359

Senescence-associated secretory phenotypes in rat-derived dedifferentiated fat cells with replicative senescence

Wenqi DENG[1], Jun-ichiro JO[2], Hidetoshi MORIKUNI[1], Satoshi SASAYAMA[3], Yoshiya HASHIMOTO[2], Naoyuki MATSUMOTO[1] and Yoshitomo HONDA[4]

[1] *Department of Orthodontics, Osaka Dental University, 8-1 Kuzuhahanazono-cho, Hirakata, Osaka 573-1121, Japan*
[2] *Department of Biomaterials, Osaka Dental University, 8-1 Kuzuhahanazono-cho, Hirakata, Osaka 573-1121, Japan*
[3] *Department of Oral Implantology, Osaka Dental University, 8-1 Kuzuhahanazono-cho, Hirakata, Osaka 573-1121, Japan*
[4] *Department of Oral Anatomy, Osaka Dental University, 8-1 Kuzuhahanazono-cho, Hirakata, Osaka 573-1121, Japan*
Corresponding author, Jun-ichiro JO; E-mail: jo-j@cc.osaka-dent.ac.jp

Senescence-associated secretory phenotype (SASPs) secreted from senescent cells often cause the deleterious damages to the surrounding tissues. Although dedifferentiated fat (DFAT) cells prepared are considered a promising cell source for regenerative therapies, SASPs from DFAT cells undergoing long-term cell culture, which latently induce replicative senescence, have barely been explored. The present study was designed to investigate senescent behaviors in rat-derived DFAT cells at high passage numbers and to analyze the possible types of SASPs. Our data show that DFAT cells undergo senescence during replicative passaging, as determined by multiple senescent hallmarks including morphological changes in cell shape and nucleus. Moreover, RT^2 PCR array analysis indicated that senescent DFAT cells expressed higher levels of 16 inflammatory cytokines (*Ccl11*, *Ccl12*, *Ccl21*, *Ccl5*, *Csf2*, *Cxcl1*, *Cxcl12*, *Ifna2*, *IL11*, *IL12a*, *IL13*, *IL1a*, *IL1rn*, *IL6*, *Mif*, and *Tnf*) associated with SASPs than non-senescent cells. This study implicates that rat DFAT cells undergo cellular senescence after long-term cell culture; cautious consideration should be paid to treat SASP secretion when senescent DFAT cells are used in regenerative medicine.

Keywords: Dedifferentiated fat cell, Cellular senescence, Senescence-associated secretory phenotypes

INTRODUCTION

Maxillofacial defects are caused by congenital anomalies (*e.g.*, cleft palate), inflammation, trauma, or tumors[1,2]. Regenerative therapy using stem cells or multipotent progenitor cells is considered as a promising approach to launch such therapies[3]. In general, cell-based regenerative medicine requires procurement of a sufficient number of cells[4]. Expanding cells by subjecting them to repetitive passaging in cell culture *in vitro* is necessary and unavoidable, and this passaging process has been shown to induce replicative senescence in stem/multipotent progenitor cells[5-7].

Cellular senescence is characterized by the irreversible arrest of cell proliferation accompanied by morphological changes of cell morphology[8]. The modes of senescence are roughly distinguished into replicative senescence, oncogene-induced senescence, and stress-induced premature senescence according to respective triggers[9]. Classically, telomere shortening associated with cell proliferation is thought to cause replicative senescence[10]. Stress-induced premature senescence is triggered by DNA damage induced by a wide variety of stressors, such as reactive oxygen species, irradiation, *etc.*[11,12]. In 2008, several research groups advocated the concept of senescence-associated secretory phenotypes (SASPs)[13-15], which were later identified to contain various pro-inflammatory factors, miRNAs, and proteases[16]. Although cytokines and chemokines are the basic and common components of SASPs, SASPs are still found to be different from the types and origins of cells[16,17]. Studies on cellular senescence have revealed that SASPs are associated with various chronic diseases, wound healing, and development[16,18].

Dedifferentiated fat (DFAT) cells derived from adipose tissue are considered a promising cell source for highly practical regenerative medicine[19,20]. DFAT cells have multilineage differentiation potential, such as adipogenic, osteogenic, and chondrogenic differentiation, similar to bone-marrow derived mesenchymal stem cells (BMSCs)[20], dental pulp stem cells[21], and adipose-derived stem cells (ADSCs)[22]. In addition, DFAT cells can be harvested less invasively than BMSCs can be, regardless of donor age or underlying diseases[23]. Moreover, homogeneous cells of higher purity are easily obtained during the isolation of DFAT cells than during that of ADSCs as smooth muscle cells and vascular endothelial cells rarely get attached to the flask through the ceiling culture[24]. Despite a variety of studies on the promising abilities of DFAT cells exploitable in regenerative medicine, little is known about SASP factors secreted from senescent rat-derived DFAT cells cultured for long term. Thus, this research aims at exploring the possible SASP factors secreted from senescent DFAT cells comprehensively. In view of the deleterious effects of SASPs on inflammation and cytotoxicity[16,25], the investigation of the SASPs of senescent DFAT cells is valuable to step forward the cell-based therapies. Therefore, in this study, we prepared senescent DFAT cells after long-term cell culture with repetitive passages and evaluated the mRNA expression of inflammatory cytokines categorized as SASPs using PCR arrays.

Received Oct 28, 2022: Accepted Nov 18, 2022
doi:10.4012/dmj.2022-242 JOI JST.JSTAGE/dmj/2022-242

MATERIALS AND METHODS

Isolation and preparation of DFAT cells

Animal experimental procedures for isolating DFAT cells by the ceiling culture method reported previously[26,27] (Fig. 1A) were approved by the Ethics Committee of Osaka Dental University (Approval No.22-02033) and strictly complied. Fat tissues (1 g) from the groin femurs of Fisher F344 rats (male, 8-week-old, Shimizu Laboratory Supplies, Kyoto, Japan) were collected and digested at 37°C for 1 h with 4-(2-hydroxyethyl)-1-piperazineethanesulfonic acid (HEPES)-Dulbecco's modified essential medium (DMEM; Invitrogen, Carlsbad, CA, USA) solution including bovine serum albumin (2%) and collagenase (0.1%) using a thermostatic shaker (BIO-Shaker BR-40LF, TAITEC, Saitama, Japan). After digestion and subsequent filtration through a nylon mesh followed by centrifugation (100×g for 3 min), the mature adipocytes floating in the upper layer of the filtered suspension were transferred into a culture flask fully filled with DMEM containing 20% fetal bovine serum (FBS; cat. no. SH30910.03; HyClone Laboratories, Logan, UT, USA). The bottom of flask was kept facing upwards during 1-week incubation at 37°C in 5% CO_2. Then, the flasks were inverted and further cultured by changing the medium every 4 days until the cells reached confluence. These cells were regarded as DFAT cells with passage number 1 (p1-DFAT). DFAT cells were cultured in DMEM supplemented with 10% FBS and 1% antibiotics (cat. no. 161-23181; Fujifilm Wako Pure Chemical, Osaka, Japan) in a 5% CO_2 incubator at 37°C, and repeatedly passaged at each time the cells were reached 80% confluence. Cells were named according to their passage number (*e.g.*, p3-DFAT for DFAT cells that underwent three passages). To observe cell morphology, images of p1-DFAT, p3-DFAT, p15-DFAT, p40-DFAT, and p60-DFAT cells were captured using a microscope (IX70, Olympus, Tokyo, Japan) at random with a phase-contrast mode.

Flow cytometric analysis of DFAT cells

The surface antigens on the p3-DFAT and p60-DFAT cells were characterized by flow cytometry using FACSVerse (BD Biosciences, Franklin Lakes, NJ, USA). PE-conjugated anti-CD34 (NBP2-47911PE, Novus Biologicals, Littleton, CO, USA), APC-conjugated anti-CD105 (NB500-452APC, Novus Biologicals), PE-conjugated anti-CD45 (202207, BioLegend, San Diego, CA, USA), and APC-conjugated anti-CD90 (202526, BioLegend) antibodies were used in this study. FlowJo X software (TreeStar, Ashland, OR, USA) was used for data analyses.

Cell Counting Kit-8 (CCK8) assay

CCK8 (Dojindo Laboratories, Kumamoto, Japan) was used to compare the proliferative ability of p3-DFAT and p60-DFAT cells. Cells were plated into 96 well plates (ThermoFisher Scientific, Waltham, MA, USA) at

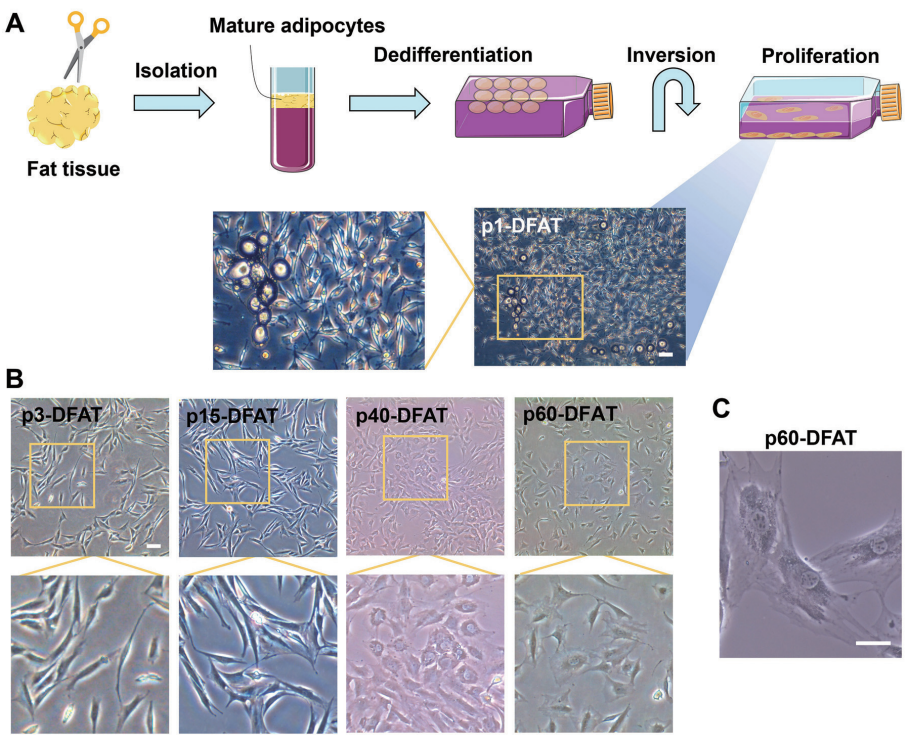

Fig. 1 (A) Schematic diagram of preparation procedures of rat-derived DFAT cells and microscopic images of DFAT cells with the passage number of 1 (p1-DFAT). (B) and (C) Phase-contrast microscopic images of DFAT cells with different passage numbers. Scale bar is 100 μm.

an initial density of 3×10^3 cells/well. Working solution of CCK8 was added to the cells immediately or at 24, 48, and 72 h after seeding and incubated for 2 h at 37°C. The absorbance of each well at 450 nm was measured using a plate reader (SpectraMax M5, Molecular Devices, Tokyo, Japan).

Senescence-associated beta-galactosidase (SA-β-Gal) staining
p3-DFAT and p60-DFAT cells were separately seeded in triplicate in 24-well plates. After 48 h, SA-β-Gal activity was determined using a senescence detection kit (ab65351, Abcam, Cambridge, MA, USA). Images were randomly acquired at 10× magnification using an Olympus IX70 microscope (Olympus) in the bright field mode.

Real-time polymerase chain reaction (RT-PCR) analysis
The total RNA of p3-DFAT and p60-DFAT was extracted using an RNeasy Mini Kit (QIAGEN, Hilden, Germany) according to the manufacturer's protocol. cDNA was synthesized from total RNA (500 ng) using the SuperScript® VILO™ cDNA synthesis kit (Thermo Fisher Scientific). PCR was performed using the One Step Plus PCR system under the following conditions. Thermal cycling conditions (cycle number: 40): 2 min at 50°C, 20 s at 95°C, 1 s at 95°C, and 20 s at 60°C. The glyceraldehyde 3-phosphate dehydrogenase (GAPDH) gene (rat GAPDH endogenous control; Thermo Fisher Scientific) was used as the internal standard. Gene expression levels were calculated using the ΔΔCT method. The experiment was repeated thrice. The accession numbers of the TaqMan probes were Rn00589996_m1(Cdkn1a), and Rn00580664_m1(Cdkn2a).

Immunofluorescent staining
The p3-DFAT and p60-DFAT cells were fixed in 4% paraformaldehyde (PFA; Fujifilm Wako Pure Chemical) for 15 min at 25°C. The cells were blocked and permeabilized with phosphate-buffered saline (PBS) containing 5% goat serum (cat. no. S-1000; Vector Laboratories, Burlingame, CA, USA) and 0.1% Triton X-100 (Sigma Aldrich, St Louis, MO, USA) for 20 min. Thereafter the cells were incubated with each antibody overnight at 4°C. The antibodies (Bioss Antibodies, Woburn, MA, USA) were as follows: Alexa Fluor® 555-conjugated anti-CDKN1A/p21 polyclonal antibody (bs-10129R-A555), and Alexa Fluor® 555-conjugated anti-CDKN2A/p16-INK4a polyclonal antibody (bs-20656R-A555). Finally, the nuclei were co-stained with DAPI Fluoromount-G® (Southern Biotechnology Associates, Birmingham, AL, USA). Staining with an antibody for urokinase-type plasminogen activator receptor (uPAR) (NBP290454AF647, Novus Biologicals) was performed using the same procedure, except for that no permeabilization that was carried out. In addition, DNA damage detection kit (γH2AX-Green G265, Dojindo Laboratories) was used for immunofluorescence staining of γH2AX in p3-DFAT and p60-DFAT cells, according to the manufacturer's instructions.

Images were captured using a fluorescence microscope (BZ-9000; Keyence, Osaka, Japan). The stained cells were quantified in four random fields using ImageJ software (1.50d, NIH Image, Bethesda, MD, USA) and expressed as the percentage of stained (positive) cells to total cells.

Nucleus staining
The p3-DFAT and p60-DFAT cells were fixed in 4% PFA for 15 min at room temperature. DAPI Fluoromount-G® was then added to the stained cell nuclei. Images were captured using a fluorescence microscope and the area of 50 DAPI-stained nuclei in each group was measured using ImageJ software.

RT² profiler PCR array analysis
Rat cytokine and chemokine RT² Profiler PCR Array (cat. no. 330231 PARN-150ZA, Qiagen) was used to analyze the expression of SASP-related genes in confluent p3-DFAT (control group) and p60-DFAT cells (experimental group) cultured in 48-well plates for 3 days. The vendor web-based software module was used to determine and analyze the relative expression of each gene. The experiments were repeated in triplicate for each group.

Statistical analysis
Statistical significance was evaluated by Student's *t*-test using the GraphPad Prism 8 software (La Jolla, CA, USA). Data are expressed as the mean±SD or mean of at least three independent experiments and were considered statistically significant when the *p*-value was less than 0.05.

RESULTS

Preparation of DFAT cells with different passage numbers
DFAT cells were isolated from the fat tissue of rats and prepared using the ceiling culture technique. Immediately after the ceiling culture, the adhered cells showed fibroblast-like morphology (Fig. 1A). DFAT cells at different passage numbers were obtained by repeated subculturing. DFAT cell morphology changed from a spindle shape to a flattened shape with vacuolated structures as the passage number increased (Figs. 1B and C). Flow cytometric analysis revealed no difference between the expression patterns of cell surface antigens on p3-DFAT and those on p60-DFAT cells (Fig. 2). Further, DFAT cells with passage numbers 3 (p3-DFAT) and 6 (p60-DFAT) were used as explained below to explore the biological properties after replicative senescence.

Senescent behaviors of DFAT cells after repeated subculture
The senescent behaviors of p3- and p60-DFAT cells were evaluated through several examinations. First, the proliferation profiles of the cells were evaluated (Fig. 3). Both p3- and p60-DFAT cells proliferated over time, the p60-DFAT cells proliferated slower than the p3-DFAT cells, suggesting that the proliferation activity of

DFAT cells decreased with increasing passage number. Secondly, senescence markers expressed in the cytosol of p3- and p60-DFAT cells were detected (Fig. 4). The p60-DFAT cells had higher SA-β-gal activity than p3-DFAT cells (Fig. 4A). The expression levels of *cdkn1a* and *cdkn2a* were higher in p60-DFAT cells than in p3-DFAT cells (Fig. 4B). Immunofluorescence staining revealed that the expression levels of senescence-related cytosolic proteins (p21 and p16) in p60-DFAT cells were significantly higher than those in p3-DFAT cells (Figs. 4C–F). Third, the expression of uPAR, a senescentce-related protein present on the cell surface, was evaluated using immunofluorescence staining. p60-DFAT cells expressed significantly greater uPAR than p3-DFAT cells (Fig. 5). Fourth, changes in the nuclei of DFAT cells associated with repeated subculture were explored (Fig.

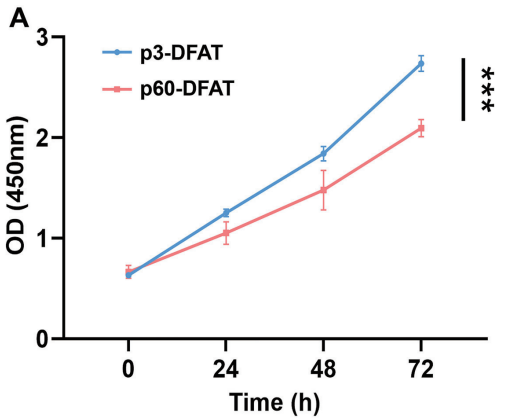

Fig. 3 Proliferation profiles of p3-DFAT and p60-DFAT cells (n=3).

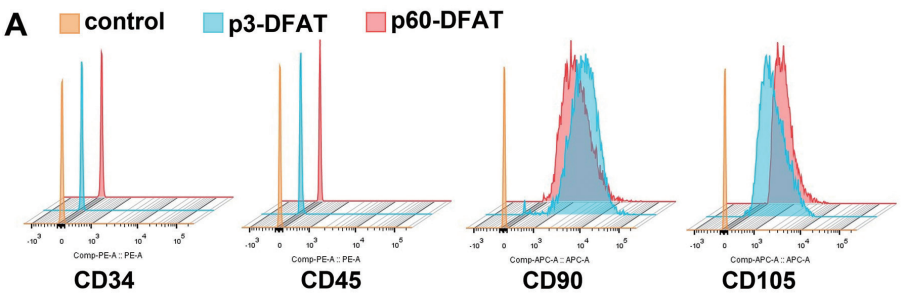

Fig. 2 Expression patterns of surface antigens (CD34, CD45, CD90, and CD105) on DFAT cells with passage numbers 3 (p3-DFAT) or 60 (p60-DFAT) evaluated by the flow cytometry.

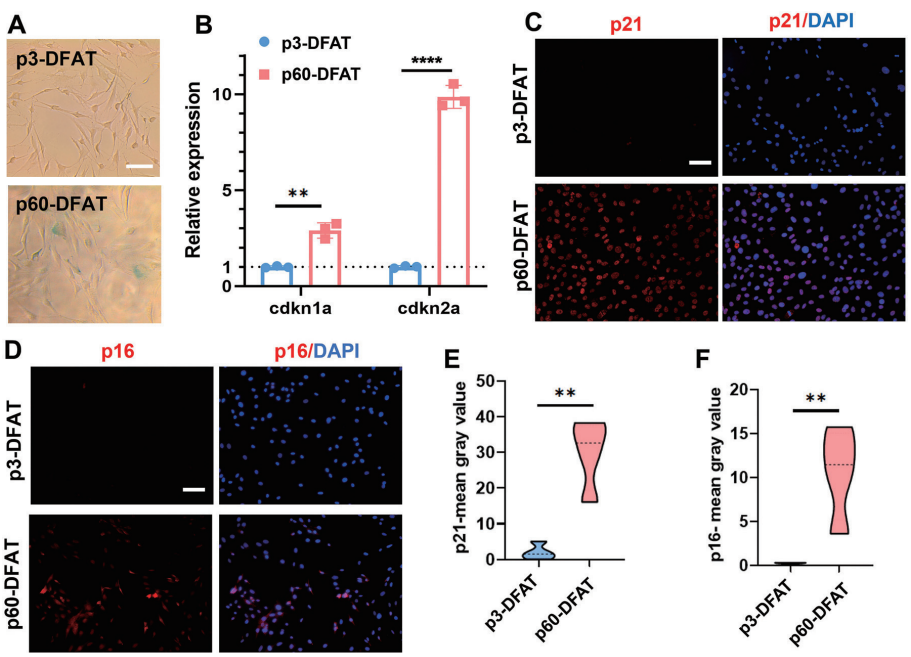

Fig. 4 Senescent markers expressed in the cytosol of p3-DFAT and p60-DFAT cells.
(A) Representative images of SA-β-gal staining. (B) Relative gene expression evaluated by RT-qPCR (n=3). (C–F) Representative immunofluorescent staining images for p21 (C) and p16 (D) and their semi-quantitation (E and F, violin plot, n=4) with mean gray value. Nucleus were co-stained with DAPI. Scale bar is 100 μm. **p<0.01, ***p<0.001.

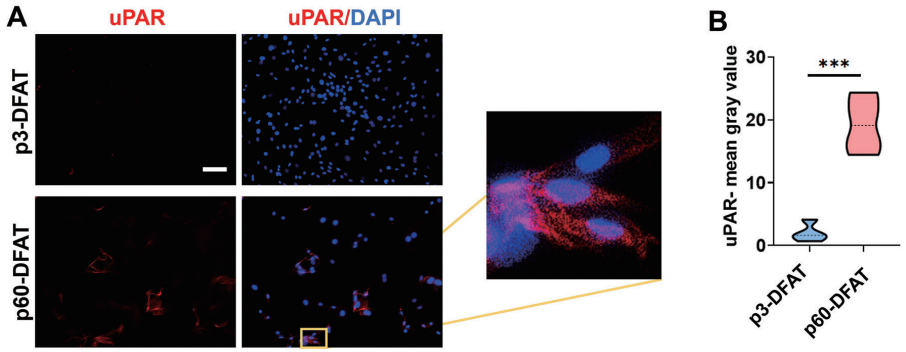

Fig. 5 A senescent marker (uPAR) expressed on the surface of p3-DFAT and p60-DFAT cells. Representative immunofluorescent staining image (A) and its semi-quantitation (B, violin plot, n=4) with mean gray value. Nucleus were co-stained with DAPI. Scale bar is 100 μm. ***p<0.001.

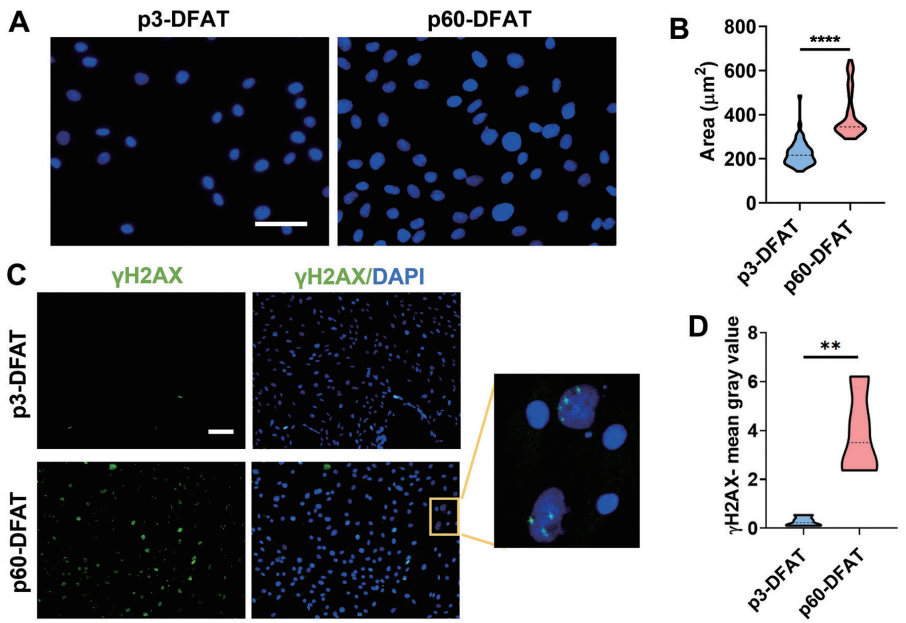

Fig. 6 Changes in the nucleus of p3-DFAT and p60-DFAT cells. (A) Representative images of nucleus stained with DAPI. (B) Semi-quantification (violin plot, n=50) with nucleus area. (C–D) Representative immunofluorescent staining images for γH2AX (C) and its semi-quantitation (D, violin plot, n=4) with mean gray value. Nucleus were co-stained with DAPI. Scale bar is 100 μm. **p<0.01, ****p<0.0001.

6). The nuclei of p60-DFAT cells were larger than those of p3-DFAT cells (Figs. 6A and B). Expression of γH2AX protein, which is related to nuclear DNA breaks, was higher in p60-DFAT cells than in p3-DFAT cells (Figs. 6C and D). These results clearly demonstrated that DFAT cells undergo cellular senescence after repeated subculturing.

Exploration of possible SASP

Based on these results, p3- and p60-DFAT cells were regarded as non-senescent and senescent cells, respectively. The possible SASPs were explored by comparing the gene expression levels between non-senescent and senescent cells using the rat cytokine and chemokine RT^2 profiler PCR array (Fig. 7). The array used in this study included 84 inflammatory factors that can be categorized as chemokines, growth factors, TNF superfamily members, interleukins, and cytokines. The expression levels of many genes were altered by replicative senescence (Fig. 7A). These results were analyzed based on expression differences (Fig. 7B), and the following 16 genes were upregulated in senescent DFAT cells (p60-DFAT) compared to their expression in non-senescent DFAT cell with fold-change more than 2 and a significant p-value (Fig. 7C): chemokine (C-C motif) ligand 11(Ccl11), chemokine (C-C motif) ligand 12 (Ccl12), chemokine (C-C motif) ligand 21 (Ccl21), chemokine (C-C motif) ligand 5 (Ccl5), colony stimulating factor 2 (Csf2), chemokine (C-X-C motif) ligand 11 (Cxcl1), chemokine (C-X-C motif) ligand 12 (Cxcl12), interferon

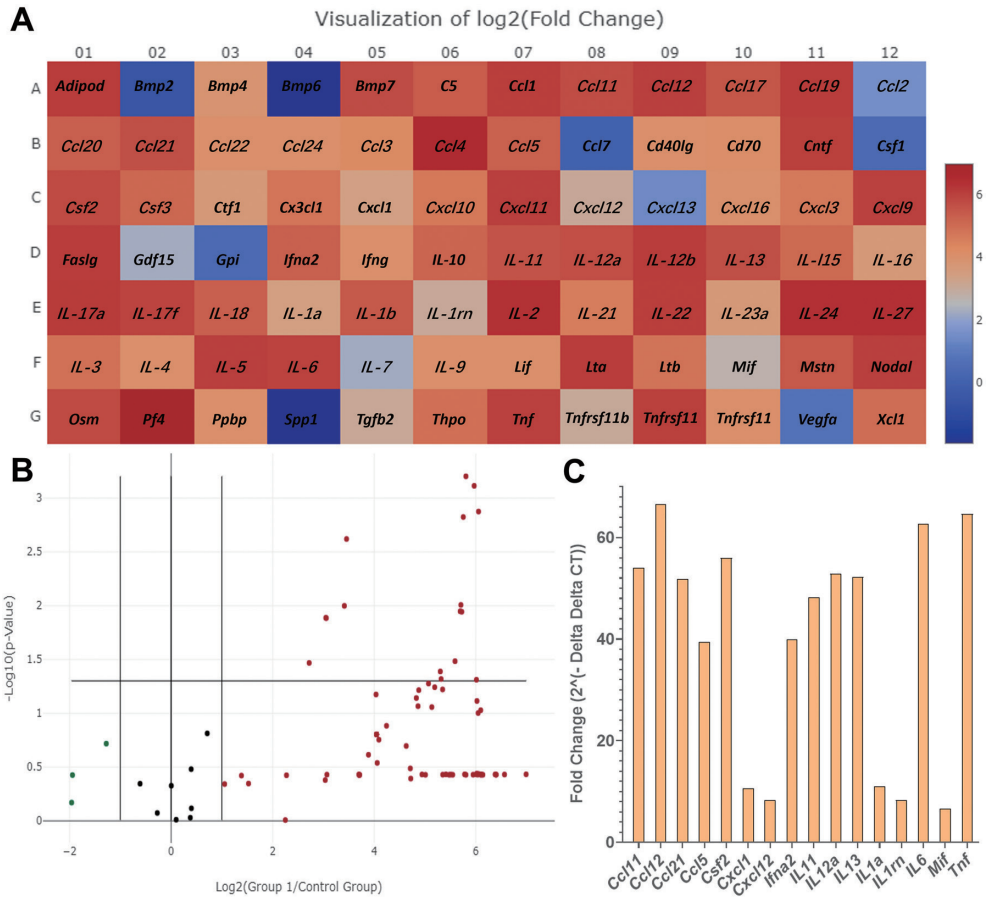

Fig. 7 (A) Heat map of relative gene expression in DFAT cells.
Relative gene expression level of p60-DFAT cells to p3-DFAT cells was evaluated by the cytokine and chemokine RT^2 profiler PCR array. Levels of gene expression relatively up-regulated and down-regulated are indicated in warm and cool colors, respectively. (B) The volcano plot of gene expression level in p60-DFAT cells (group 1) relative to p3-DFAT cells (control group). Yellow, blue, and black plots indicate up-regulated (difference: >2-fold), down-regulated (difference: >2-fold), and non-differentially expressed genes (difference: ≤2-fold), respectively. (C) Bar chart of genes with fold-change greater than 2 and significant statistical (p<0.05) differences. The genes plotted in the upper-right corner of Fig. 7B. Data is expressed as the mean of observations (n=3).

alpha 2 (Ifna2), interleukin 11 (IL11), interleukin 12a (IL12a), interleukin 13 (IL13), interleukin 1 alpha (IL1a), interleukin 1 receptor antagonist (IL1rn), interleukin 6 (IL6), macrophage migration inhibitory factor (Mif), and tumor necrosis factor (Tnf).

DISCUSSION

Advances in cell therapy have widened the use of various multipotent stem or progenitor cells, including DFAT cells[28]. Nevertheless, information regarding the replicative senescence and SASP behavior of rat DFAT cells is scarce. In this study, we demonstrated that cells cultured for up to 60 passages provoked cellular senescence, leading to elevated expression of mRNAs, encoding numerous inflammatory cytokines associated with SASP factors.

Senescent markers are known to show heterogeneity in senescent cells, depending on the cell type, origin, and senescence stage[29,30]. Cellular senescence is commonly verified using a variety of senescent markers and other hallmarks[8,31]. Additionally, senescent cells generally change their cell[8] and nuclear shape[32]. In our data, there was a negligible difference in the cell surface antigens (CD 90 and 105) representative markers of DFAT cells[33] up to passage 60 (Figs. 2 and 3) and slight attenuation of cell growth. However, we could confirm cellular senescence in p60 cells using a variety of representative senescence markers such as SA-β-Gal, p21, p16, and uPAR (Figs. 4 and 5). In addition to the expression changes of these markers, morphological changes were also observed in p60-DFAT cells that gradually got flattened with enlarged nuclear. These results indicated that DFAT undergoes replicative senescence when expanded *in vitro*.

p21, encoded by the CDKN1A gene, leads to cell cycle arrest at G1/S when highly expressed[34]; p16, encoded by the CDK2A gene, has been reported to be significant

in maintaining irreversible growth arrest[35]. Our data showed that p60-DFAT cells expressed both p21 and p16, as evident from PCR assay and immunofluorescence staining (Fig. 4). Nevertheless, cell proliferation ability was retained even in DFAT cells after long-term cell culture up to passage 60. Other porcine DFAT cells also exhibit similar resistance to long-term cell culture[36]. Meanwhile, other stem cells (*e.g.*, ADSCs) or progenitor cells readily lose their proliferative ability after long-term cell cultures[37]. Given these results, DFAT cells may have resistance mechanisms to evade cell cycle arrest when subjected to cellular senescence. In addition to the decrement of proliferative capacity, the cellular senescence impairs the capacity to differentiate stem cells[38]. MSCs have diminished the osteogenic differentiation potential with increasing passage numbers *in vitro*[39]. Our other unpublished findings also show that senescent DFAT cells do not escape the decline in osteogenic differentiation.

Although the relationship between replicative senescence and stress-induced premature senescence is controversial in the long history of cellular senescence study[11], replicative senescence has been categorized differently from stress-induced premature senescence[40]. Indeed, other researchers have reported that replicative senescence can be distinguished from induced senescence by analyzing rDNA or methylation of its promoter[41]. Telomerase shortening, the main phenotype of cell replication, is thought to be the main trigger for inducing replicative senescence[42,43]. Recently, various studies have shown that telomere shortening causes constant DNA damage response, leading to stress-induced premature senescence[44]. Other researchers have shown that the substrate stiffness of the culture surface modifies the degree of cellular senescence; hydrogel stiffness reduces replicative senescence in MSCs[45]. In our study, we found more cells with γH2AX-positive nuclear DNA damage in p60-DFAT cells than in p3-DFAT cells. However, the damage was not present in all 60-DFAT cells, although most of them expressed p21, a well-known marker for senescence. We presume that p60-DFAT cells might undergo cellular senescence by telomere shortening and receive stress from the stiffness of the cell culture plates albeit not analyze the telomere shortening in this study.

SASP factors secreted from senescent cells not only reinforce senescence in their own *via* autocrine signaling but also affect adjacent cells and even alter the local microenvironment into an inflammatory niche through paracrine effects[46]. In our study, p60-DFAT cells secreted more cytokines than p3-DFAT cells as shown by the RT^2-PCR array analysis. The up-regulated genes with statistical significance could be broadly classified into the following categories: interleukins (*IL-11*, *IL-1a*, *IL-12a*, *IL-13*, *IL-1rn*, *IL-11*, and *IL-6*), chemokines (*Mif*, *Ccl5*, *Ccl11*, *Ccl12*, *Ccl21*, *Cxcl1*, and *Cxcl12*), growth factors (*Csf2*), TNF family (*Tnf*), and other cytokines (*Ifna2*). All of their downstream proteins have been recognized as SASPs in a previous study[47]. Among them, *IL-1a* and *IL-6* have been reported to enhance the senescent state through autonomous action[35]. *Csf-2*, *IL-11*, *IL-13*, *IL-1a*, *IL-6* and *TNF* are involved in DNA damage-induced senescence[35].

SASPs have been considered a double-edged sword that mediates several pathological and physiological effects in senescent cells[18]. Some SASP secretions occasionally function as crucial factors for wound healing[48] and development[49]. Acute short exposure to SASPs has been shown to promote regeneration through induction of cell plasticity and stemness[50]. In contrast, chronic accumulation of SASP factors can lead to negative results[50]. Those molecules damaged the surrounding tissues, hampering tissue regeneration processes such as bone formation[51,52]. Based on the complexity of SASPs, more specific experiments would be essential to clarify how SASP factors from DFAT cells that affect the host *in vivo*. Since the PCR array performed in this study is limited to evaluating the expression profiles at the mRNA level, the main limitation of this study is the lack of information on how the secreted SASPs interact with surrounding cells, which needs to clarified in the future investigation. However, the comprehensive data from our PCR array analysis may provide valuable insights to estimate the properties of senescent DFAT cells.

CONCLUSION

In this study, we investigated the characteristics of replicative senescent DFAT cells after long-term cell culture up to passage number 60 and comprehensively analyzed the changes in the SASP factors secreted from the cells. Our study indicates that DFAT also undergoes cellular senescence during continuous passage of cultures and may secrete various types of SASP factors. We could not find p21- and p16-positive cells at passage three, while p60-DFAT exhibited stable characteristic surface antigens and senescence markers (p21, p16, and uPAR), suggesting that DFAT cells became senescent after the passages. Additionally, p60-DFAT cells had larger nuclei than p3-DFAT cells did. γH2AX-positive nuclei were detected, indicating that the cells partially underwent DNA damage after long-term cell culture. During the PCR array analysis, numerous mRNAs encoding inflammatory cytokines (*i.e.*, IL-6, TNF) and chemokines (*i.e.*, Ccl12) were found to be increased in p60-DFAT cells compared to those in p3-DFAT cells. These results indicate that long-term cell culture causes cellular senescence in DFAT cells, resulting in the enhanced secretion of inflammatory SASP factors. The effect of SASP secretion should be carefully considered when using prolonged-cultured DFAT for cell-based treatment.

ACKNOWLEDGMENTS

This work was partially supported by the Japan Society for the Promotion of Science (JSPS) KAKENHI grant number JP20K18587.

CONFLICT OF INTEREST

The authors declare no conflict of interest.

REFERENCES

1) Herford AS, Miller M, Signorino F. Maxillofacial defects and the use of growth factors. Oral Maxillofac Surg Clin North Am 2017; 29: 75-88.
2) Walmsley GG, Ransom RC, Zielins ER, Leavitt T, Flacco JS, Hu MS, *et al*. Stem cells in bone regeneration. Stem Cell Rev Rep 2016; 12: 524-529.
3) Holly D, Klein M, Mazreku M, Zamborsky R, Polak S, Danisovic L, *et al*. Stem cells and their derivatives-implications for alveolar bone regeneration: A comprehensive review. Int J Mol Sci 2021; 22: 11746.
4) Mao AS, Mooney DJ. Regenerative medicine: Current therapies and future directions. Proc Natl Acad Sci U S A. 2015; 112: 14452-14459.
5) Christodoulou I, Kolisis FN, Papaevangeliou D, Zoumpourlis V. Comparative evaluation of human mesenchymal stem cells of fetal (Wharton's jelly) and adult (adipose tissue) origin during prolonged *in vitro* expansion: Considerations for cytotherapy. Stem Cells Int 2013; 2013: 246134.
6) Kim SN, Choi B, Lee CJ, Moon JH, Kim MK, Chung E, *et al*. Culturing at low cell density delays cellular senescence of human bone marrow-derived mesenchymal stem cells in long-term cultures. Int J Stem Cells 2021; 14: 103-111.
7) Morsczeck C. Cellular senescence in dental pulp stem cells. Arch Oral Biol 2019; 99: 150-155.
8) Mohamad Kamal NS, Safuan S, Shamsuddin S, Foroozandeh P. Aging of the cells: Insight into cellular senescence and detection Methods. Eur J Cell Biol 2020; 99: 151108.
9) Lunyak VV, Amaro-Ortiz A, Gaur M. Mesenchymal stem cells secretory responses: Senescence messaging secretome and immunomodulation perspective. Front Genet 2017; 8: 220.
10) Herbig U, Jobling WA, Chen BP, Chen DJ, Sedivy JM. Telomere shortening triggers senescence of human cells through a pathway involving ATM, p53, and p21(CIP1), but not p16(INK4a). Mol Cell 2004; 14: 501-513.
11) Suzuki M, Boothman DA. Stress-induced premature senescence (SIPS) —Influence of SIPS on radiotherapy. J Radiat Res 2008; 49: 105-112.
12) Toussaint O, Remacle J, Dierick JF, Pascal T, Frippiat C, Royer V, *et al*. Stress-induced premature senescence: From biomarkers to likeliness of in vivo occurrence. Biogerontology 2002; 3: 13-17.
13) Acosta JC, O'Loghlen A, Banito A, Guijarro MV, Augert A, Raguz S, *et al*. Chemokine signaling via the CXCR2 receptor reinforces senescence. Cell 2008; 133: 1006-1018.
14) Kuilman T, Michaloglou C, Vredeveld LC, Douma S, van Doorn R, Desmet CJ, *et al*. Oncogene-induced senescence relayed by an interleukin-dependent inflammatory network. Cell 2008; 133: 1019-1031.
15) Wajapeyee N, Serra RW, Zhu X, Mahalingam M, Green MR. Oncogenic BRAF induces senescence and apoptosis through pathways mediated by the secreted protein IGFBP7. Cell 2008; 132: 363-374.
16) Birch J, Gil J. Senescence and the SASP: Many therapeutic avenues. Genes Dev 2020; 34: 1565-1576.
17) Rodier F, Campisi J. Four faces of cellular senescence. J Cell Biol 2011; 192: 547-556.
18) Lopes-Paciencia S, Saint-Germain E, Rowell MC, Ruiz AF, Kalegari P, Ferbeyre G. The senescence-associated secretory phenotype and its regulation. Cytokine 2019; 117: 15-22.
19) Kishimoto N, Honda Y, Momota Y, Tran SD. Dedifferentiated fat (DFAT) cells: A cell source for oral and maxillofacial tissue engineering. Oral Dis 2018; 24: 1161-1167.
20) Shen JF, Sugawara A, Yamashita J, Ogura H, Sato S. Dedifferentiated fat cells: An alternative source of adult multipotent cells from the adipose tissues. Int J Oral Sci 2011; 3: 117-124.
21) Gioventu S, Andriolo G, Bonino F, Frasca S, Lazzari L, Montelatici E, *et al*. A novel method for banking dental pulp stem cells. Transfus Apher Sci 2012; 47: 199-206.
22) Huang G, Xia B, Dai Z, Yang R, Chen R, Yang H. Comparative study of dedifferentiated fat cell and adipose-derived stromal cell sheets for periodontal tissue regeneration: In vivo and in vitro evidence. J Clin Periodontol 2022; 49: 1289-1303.
23) Nakayama E, Matsumoto T, Kazama T, Kano K, Tokuhashi Y. Transplantation of dedifferentiation fat cells promotes intervertebral disc regeneration in a rat intervertebral disc degeneration model. Biochem Biophys Res Commun 2017; 493: 1004-1009.
24) Matsumoto T, Kano K, Kondo D, Fukuda N, Iribe Y, Tanaka N, *et al*. Mature adipocyte-derived dedifferentiated fat cells exhibit multilineage potential. J Cell Physiol 2008; 215: 210-222.
25) Zhang L, Pitcher LE, Prahalad V, Niedernhofer LJ, Robbins PD. Targeting cellular senescence with senotherapeutics: Senolytics and senomorphics. FEBS J 2023; 290: 1362-1383.
26) Sasayama S, Hara T, Tanaka T, Honda Y, Baba S. Osteogenesis of multipotent progenitor cells using the epigallocatechin gallate-modified gelatin sponge scaffold in the rat congenital cleft-jaw model. Int J Mol Sci 2018; 19: 3803.
27) Nakano K, Kubo H, Nakajima M, Honda Y, Hashimoto Y. Bone regeneration using rat-derived dedifferentiated fat cells combined with activated platelet-rich plasma. Materials (Basel) 2020; 13: 5097.
28) Ong WK, Chakraborty S, Sugii S. Adipose tissue: Understanding the heterogeneity of stem cells for regenerative medicine. Biomolecules 2021; 11: 918.
29) De Cecco M, Ito T, Petrashen AP, Elias AE, Skvir NJ, Criscione SW, *et al*. L1 drives IFN in senescent cells and promotes age-associated inflammation. Nature 2019; 566: 73-78.
30) Hernandez-Segura A, Nehme J, Demaria M. Hallmarks of cellular senescence. Trends Cell Biol 2018; 28: 436-453.
31) Dodig S, Cepelak I, Pavic I. Hallmarks of senescence and aging. Biochem Med (Zagreb) 2019; 29: 030501.
32) Pathak RU, Soujanya M, Mishra RK. Deterioration of nuclear morphology and architecture: A hallmark of senescence and aging. Ageing Res Rev 2021; 67: 101264.
33) Watson JE, Patel NA, Carter G, Moor A, Patel R, Ghansah T, *et al*. Comparison of markers and functional attributes of human adipose-derived stem cells and dedifferentiated adipocyte cells from subcutaneous fat of an obese diabetic donor. Adv Wound Care (New Rochelle) 2014; 3: 219-228.
34) Deng T, Yan G, Song X, Xie L, Zhou Y, Li J, *et al*. Deubiquitylation and stabilization of p21 by USP11 is critical for cell-cycle progression and DNA damage responses. Proc Natl Acad Sci U S A 2018; 115: 4678-4683.
35) Kumari R, Jat P. Mechanisms of cellular senescence: Cell cycle arrest and senescence associated secretory phenotype. Front Cell Dev Biol 2021; 9: 645593.
36) Peng X, Song T, Hu X, Zhou Y, Wei H, Peng J, *et al*. Phenotypic and functional properties of porcine dedifferentiated fat cells during the long-term culture in vitro. Biomed Res Int 2015; 2015: 673651.
37) Tansriratanawong K, Tabei I, Ishikawa H, Ohyama A, Toyomura J, Sato S. Characterization and comparative DNA methylation profiling of four adipogenic genes in adipose-derived stem cells and dedifferentiated fat cells from aging subjects. Hum Cell 2020; 33: 974-989.
38) Lin H, Sohn J, Shen H, Langhans MT, Tuan RS. Bone marrow mesenchymal stem cells: Aging and tissue engineering

applications to enhance bone healing. Biomaterials 2019; 203: 96-110.
39) Gu Y, Li T, Ding Y, Sun L, Tu T, Zhu W, *et al*. Changes in mesenchymal stem cells following long-term culture in vitro. Mol Med Rep 2016; 13: 5207-5215.
40) Amaya-Montoya M, Perez-Londono A, Guatibonza-Garcia V, Vargas-Villanueva A, Mendivil CO. Cellular senescence as a therapeutic target for age-related diseases: A review. Adv Ther 2020; 37: 1407-1424.
41) Sanokawa-Akakura R, Akakura S, Ostrakhovitch EA, Tabibzadeh S. Replicative senescence is distinguishable from DNA damage-induced senescence by increased methylation of promoter of rDNA and reduced expression of rRNA. Mech Ageing Dev 2019; 183: 111149.
42) Victorelli S, Passos JF. Telomeres and cell senescence —Size matters not. EBioMedicine 2017; 21: 14-20.
43) Martin H, Doumic M, Teixeira MT, Xu Z. Telomere shortening causes distinct cell division regimes during replicative senescence in Saccharomyces cerevisiae. Cell Biosci 2021; 11: 180.
44) Fumagalli M, Rossiello F, Clerici M, Barozzi S, Cittaro D, Kaplunov JM, *et al*. Telomeric DNA damage is irreparable and causes persistent DNA-damage-response activation. Nat Cell Biol 2012; 14: 355-365.
45) Ogle ME, Doron G, Levy MJ, Temenoff JS. Hydrogel culture surface stiffness modulates mesenchymal stromal cell secretome and alters senescence. Tissue Eng Part A 2020; 26: 1259-1271.
46) Nelson G, Wordsworth J, Wang C, Jurk D, Lawless C, Martin-Ruiz C, *et al*. A senescent cell bystander effect: Senescence-induced senescence. Aging Cell 2012; 11: 345-349.
47) Xu L, Wang Y, Wang J, Zhai J, Ren L, Zhu G. Radiation-induced osteocyte senescence alters bone marrow mesenchymal stem cell differentiation potential via paracrine signaling. Int J Mol Sci 2021; 22: 9323.
48) Demaria M, Ohtani N, Youssef SA, Rodier F, Toussaint W, Mitchell JR, *et al*. An essential role for senescent cells in optimal wound healing through secretion of PDGF-AA. Dev Cell 2014; 31: 722-733.
49) Storer M, Mas A, Robert-Moreno A, Pecoraro M, Ortells MC, Di Giacomo V, *et al*. Senescence is a developmental mechanism that contributes to embryonic growth and patterning. Cell 2013; 155: 1119-1130.
50) Ritschka B, Storer M, Mas A, Heinzmann F, Ortells MC, Morton JP, *et al*. The senescence-associated secretory phenotype induces cellular plasticity and tissue regeneration. Genes Dev 2017; 31: 172-183.
51) Huang A, Honda Y, Li P, Tanaka T, Baba S. Integration of epigallocatechin gallate in gelatin sponges attenuates matrix metalloproteinase-dependent degradation and increases bone formation. Int J Mol Sci 2019; 20: 6042.
52) Ambrosi TH, Marecic O, McArdle A, Sinha R, Gulati GS, Tong X, *et al*. Aged skeletal stem cells generate an inflammatory degenerative niche. Nature 2021; 597: 256-262.